ELSEVIER

Contents lists available at ScienceDirect

Chemosphere

journal homepage: www.elsevier.com/locate/chemosphere



Check for updates

A laboratory rill study of IMX-104 transport in overland flow

Benjamin Karls ^{a,*}, Stephen Mercer Meding ^b, Li Li ^c, Viktor Polyakov ^d, Warren Kadoya ^e, Samuel Beal ^e, Katerina Dontsova ^{b,**}

- ^a University of Arizona Department of Environmental Science, 1177 E. 4th Street, Tucson, AZ, 85721, USA
- ^b University of Arizona Biosphere 2, 32540 S Biosphere Rd, Oracle, AZ, 85739, USA
- ^c Changjiang River Scientific Research Institute of Changjiang Water Resources Commission, Wuhan, 430010, China
- ^d USDA Southwest Watershed Research Center, 2000 E Allen RD, Tucson, AZ, 85719, USA
- ^e U.S. Army Engineer Research and Development Center (ERDC), Cold Regions Research and Engineering Laboratory (CRREL), 72 Lyme Road, Hanover, NH, 03755-1290, USA

HIGHLIGHTS

- Particle size had significant impact on the amount of DNAN, RDX, HMX, and NTO transported in sediment and solution.
- Flow rate had a significant impact on the amount of DNAN, RDX, HMX, and NTO transported in sediment.
- Flow rate and particle size had a significant impact on the amount of DNAN, RDX, HMX, and NTO remaining on the surface.
- NTO transports greater in solution where RDX, HMX, DNAN were more likely to be found transported with the sediment.

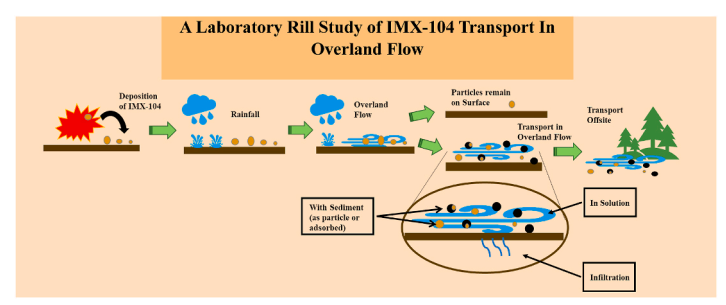
ARTICLE INFO

Handling Editor: Keith Maruya

Keywords: IMX-104 Overland flow Transport Dissolution Rill

GRAPHICAL ABSTRACT

Visual depiction of the transport of IMX-104 in overland flow and its potential transport pathways.



ABSTRACT

The deposition of explosive contaminants in particulate form onto the soil surface during low-order detonations can lead to ground and surface water contamination. The vertical fate and transport of insensitive munitions formulation IMX-104 through soil has been thoroughly studied, however the lateral transport of explosive particles on the surface is less known. The objective of this research was to understand the impact of overland flow on the transport of IMX-104 constituent compounds 3-nitro-1,2,4-triazol-5-one (NTO), 2,4-dinitroanisole (DNAN), hexahydro-1,3,5-trinitro-1,3,5-triazine (RDX), and octahydro-1,3,5,7-tetranitro-1,3,5,7-tetrazocine (HMX). The effect of overland flow was examined in a rill flume using several flow rates (165-, 265-, and 300-mL min⁻¹) and IMX-104 particle sizes (4.75–9.51 mm, 2.83–4.75 mm, 2–2.83 mm, and <2 mm). We found that the smaller particles were transported more in solution and with the sediment compared to the larger particles, which had a higher percent mass remaining on the surface. As flow rate increased, there was an increase in the percent mass found in solution and sediment and a decrease in the percent mass remaining on the surface. NTO fate was dominated by transport in solution, while DNAN, RDX and HMX were predominantly

^{*} Corresponding author. 127 S. 5th Ave APT 413, Tucson, AZ, 85701, USA.

^{**} Corresponding author. 1177 E 4th St RM 515, Tucson, AZ, 85719, USA.

E-mail addresses: benjaminkarls@email.arizona.edu (B. Karls), dontsova@arizona.edu (K. Dontsova).

transported with the sediment. This research provides evidence of the role of overland flow in the fate of energetic compounds.

1. Introduction

Insensitive munitions (IM) are being introduced by the US military as alternatives to replace commonly used explosives like 2,4,6-trinitrotoluene (TNT). IM are more stable and will not detonate without anticipated stimuli. The primary IM formulations are IMX-104 and IMX-101. IMX-104 was designed to replace Composition B (Comp B) and has four constituent compounds: DNAN (2,4-dinitroanisole), NTO (3-nitro-1,2,4triazol-5-one), RDX (hexahydro-1,3,5-trinitro-1,3,5-triazine), and HMX (octahydro-1,3,5,7- tertranitro-1,3,5,7- -tetrazocine). These compounds are released as particles on soil surfaces when explosives undergo low order (LO) or incomplete detonations. Bigl et al. (2021) reported that LO detonations deposited an average of 40% of the original explosive particulates with the <2 mm fraction of particles comprising the majority of those found on the surface (71 \pm 8.1%). The transport of IMX-104 in the environment depends on the properties of these constituent compounds. These primary transport pathways are dissolution and transport through soils with infiltrating water, where energetic constituents can be adsorbed, degraded, and/or taken up by plants, and transport in overland flow in solution, as particles, and adsorbed to the sediment.

The solubilities of the constituent compounds determine their ability to be transported in solution. This could be either in overland flow or with infiltrating water. The compound with the highest solubility is NTO with a value of 16,642 mg L $^{-1}$ (Spear et al., 1989). DNAN has a solubility of 276.2 mg L $^{-1}$ (Boddu et al., 2008). RDX and HMX both have a lower solubility of 60 mg L $^{-1}$ (Brannon and Pennington, 2002) and 5 mg L $^{-1}$ (Glover and Hoffsommer, 1973), respectively. The higher solubility is expected to make NTO more mobile in the environment while RDX and HMX are more likely to be transported with the sediment.

As runoff travels down a rill, a shallow channel cut into soil by flowing water, soil sediment and particles are picked up and transported by water. Transport with sediment can occur in two forms: as individual particles of energetic formulations (most commonly resulting from LO detonations) or adsorbed to the eroding soil. DNAN readily adsorbs to soils with higher percent organic carbon (OC) and clay (Arthur et al., 2017) with a log K_{OC} of 3.11 cm³ g⁻¹ (Dontsova et al., 2014). DNAN can reversibly adsorb to organic matter and phyllosilicate clays and undergo irreversible sorption to organic matter after reduction of nitro groups (Arthur et al., 2017; Boddu et al., 2008; Dontsova et al., 2009; Hawari et al., 2015). RDX and HMX have low sorption coefficients that range widely and depend on the organic matter (OM) content of soil or sediment (Dontsova et al., 2009) but is not influenced by sorption to clay minerals (Haderlein et al., 1996), which makes them more mobile in the environment. HMX adsorbs to organic matter to a greater extent than RDX due to its larger molecular weight, lower aqueous solubility, and the extra nitro group which allows it to form stronger sorbate-carbon complexes (Kar et al., 1996). NTO was found to adsorb to soil ten times less than RDX (Mark et al., 2016), although this value depends on soil conditions. Due to the low adsorption to the soils, NTO can move rapidly into ground water (Arthur et al., 2018; Mark et al., 2017). Just as energetic compounds can adsorb to soil sediment, they can also adsorb to the soil surface.

Energetic particles that remain on the soil surface can continue to release dissolved energetic constituents over time. Released compounds move through the soil where they can experience adsorption and degradation. DNAN like other nitroaromatic compounds has high recalcitrance to oxidation and hydrolysis (Douglas et al., 2012), but is easily reduced to carcinogenic aromatic amines during biotransformation (Ju and Parales, 2010). Nitroaromatics are also susceptible to photo-and phyto-degradation (Clausen and Korte, 2011). RDX was reported to be unstable in high reducing conditions (Price et al., 2001),

while HMX was found to be recalcitrant in surface sediments allowing for it to persist longer in groundwater (Clausen and Korte, 2011). NTO concentration decreases in soils over time due to transformation which indicates the potential for natural attenuation (Arthur et al., 2018; Mark et al., 2017).

While transport of energetic constituents through soils and their transformation reactions have been studied extensively for traditional explosive formulations, and some work has been done for insensitive munitions constituents, transport in overland flow or runoff, the flow of water on the soil surface after a rainfall, has not been systematically evaluated. Fuller et al. (2015) found dissolved and solid-phase energetics in the surface runoff close to the munition testing site. Price et al. (2011), evaluated energetics transport in mesocosm flumes with various soils (clay, loam, and sandy loam) and surface conditions (bare upland soil, vegetated upland soil, and vegetated wetland soil) after rainfall. The study observed translocation of the particles downhill and found that vegetation decreased the amount of contaminants in runoff. They also performed a batch dissolution experiment with agitated suspended sediment which indicated that an increase in total suspended solids (TSS) generally increased the amount of dissolved RDX, TNT, and HMX in solution. This suggests that sediment transport can increase dissolution of the energetic particles due to abrasion. In soil column studies with particles of Comp B (RDX and TNT) and C4 (RDX and wax), Morley et al. (2006) found that, in general, as flow rates increased, dissolution and mass transfer also increased. While these studies show the potential for transport in overland flow, they do not allow to predict its extent. We can look at research on transport of other contaminants in overland flow to partially fill this gap in knowledge.

The role of overland flow in translocation on landscapes has been studied for other contaminants and chemical compounds and a significant impact of overland flow has been observed. Deng et al. (2019) compared transport of phosphorus (P) in overland flow and interflow (lateral movement of water in the unsaturated zone). Overland flow was found to be the dominant loss pathway for P, and with increased rainfall there was an increase of overland flow and transport of P. Cadwalader et al. (2011) observed that physical transport with silt-sized particles and aggregates was the primary transport vector of arsenic and P derived from pesticide-contaminated soil. Transport was enhanced by land disturbances that increased erosion, allowing for the further movement of contaminants to streams where they are more bioavailable. Hyer (2001) found that the transport of atrazine was significantly impacted by overland flow. The study states that nearly 95% of the atrazine transported from fields was sorbed to suspended sediment in overland flow. During overland flow, Guo et al. (2018) reported average flow velocity and Reynold number (ratio of fluid momentum force to viscous shear force) are good indicators of sediment transport or solute transport. These studies display the impact overland flow has on the transport of contaminants and how overland flow can contribute to the accumulation of contaminants in soil. However, unlike contaminants in these studies, energetics enter the environment as particles of formulations (Taylor et al., 2015) adding another potential mechanism for their movement in overland flow.

The controlling factors of sediment transport have been described in numerous studies. In overland flow, sediment transport capacity positively correlates with the flow discharge and slope gradient (Zhang et al., 2021). Yang (1979) found unit stream power, the rate of potential energy spent per unit weight of water, to be the best predictor for sediment transport. Bagnold (1966) defined stream power (Ω) using the following equation:

$$\Omega = \tau V = \rho_w g S q \tag{1}$$

where τ is shear stress, V is velocity of flow, ρ_w is the density of water, g is the acceleration due to gravity, S is slope, and q is overland flow discharge. Shear stress is the force per unit of wetted area acting on a surface (Yalin, 1963):

$$\tau = \rho_{w}gSh \tag{2}$$

where *h* is the hydraulic radius or height of water.

Stream power was also found by Nearing et al. (1997) and Wang et al. (2011) to be the best predictor of sediment transport, while Guo et al. (2018) reported it to be Reynolds number. Guo et al. (2018) also reported that velocity was the best predictor for total transport of solute in runoff.

To fill the knowledge gap regarding the transport of IMX-104 in overland flow, the objective of this work was to examine different mechanisms which influence how constituent compounds (DNAN, HMX, NTO, and RDX) are transported in overland flow. We hypothesize that the more soluble constituents will dissolve and subsequently move in the runoff or infiltrate down the soil profile whereas the less soluble constituents will adsorb to the soil surface or travel with the sediment.

2. Materials and methods

2.1. Materials

2.1.1. IMX-104 particles

The IMX-104 particles in this experiment were obtained from low-order detonation tests in the Environmental Security Technology Certification Program (ESTCP) project number ER18-5105. The particles were collected on ice after the detonation and separated using a standard stack of sieves. Size distribution of particles less than 2 mm in diameter was further analyzed by laser diffraction (Bigl et al., 2020). Of these, four size ranges were used in this experiment: <2 mm (very small), 2–2.83 mm (small), 2.83–4.75 mm (medium), and 4.75–9.51 mm (large). Chemical analysis of IMX-104 revealed that the <2 mm particles had lower purity compared to the other particle sizes of IMX-104 resulting in composition of DNAN, HMX, RDX, and NTO not being the same as in the other particle sizes.

2.1.2. Soil characterization

The soil used in this experiment was collected from Arizona Army National Guard Florence Military Reservation, in Florence, AZ. This soil has been classified as Laveen loam, coarse-loamy, mixed, superactive, hyperthermic Typic Haplocalcids. It was collected separately but from the same area as Florence soil used in previous studies that examined the fate of IM constituents, NTO and DNAN, as well as their formulations, IMX-101 and IMX-104 (Arthur et al., 2017, 2018; Mark et al., 2016, 2017). Soil texture for this soil was determined by pipette method (Olmstead, 1930). It was found that the soil was sandy clay loam with 29.0% clay, 14.2% silt, and 56.8% sand. This soil had an electrical conductivity (EC) of 252 μS cm $^{-1}$, a pH of 8.3, a TOC of 0.2645%, and a cation exchange capacity (CEC) of 13.71 cmol $_{\rm c}$ kg $^{-1}$.

2.1.3. Methods

The rill flumes were designed after the mini flumes used in Nearing et al. (1997) and Nouwakpo et al. (2010). The flume had a total length of 90 cm, was 6 cm wide and 16 cm deep. It had a 30-cm long V-shaped inlet and a 10-cm long outlet to prevent sediment buildup, with the 50-cm long rectangular middle section packed with the soil. The side angles on the V were 45° and the V itself was 3.8 cm deep (Fig. 1).

The flume was supported by a wooden frame that allowed the rill slope to be adjusted. The rill box was packed with 10 cm of silica sand, with the remaining volume occupied by the soil. Nylon mesh was placed above and below the sand. The mesh at the bottom prevented the sand from entering the infiltration outlets at the bottom of the box, while the mesh at the top created a permeable barrier between the sand and soil so that soil could be collected at the end of the experiment without sand. To maintain uniform density the soil was packed in three layers, two layers of 660 g of soil each, and a layer of 330 g. These weights were determined during trial runs as they allowed to pack the box consistently every replication. As the last layer was packed, a wooden block with the same shape as the metal inlet and outlet was used to form the soil surface of the rill. The outlets at the bottom of the box were connected with plastic tubing to a flask filled with water that was used to maintain the water table in the rill and collect infiltration. The soil was saturated for approximately 20 min from the bottom using reverse osmosis (RO) purified water through the drainage outlets, and then the water table was maintained at 5 cm below the soil surface. The water table was kept just

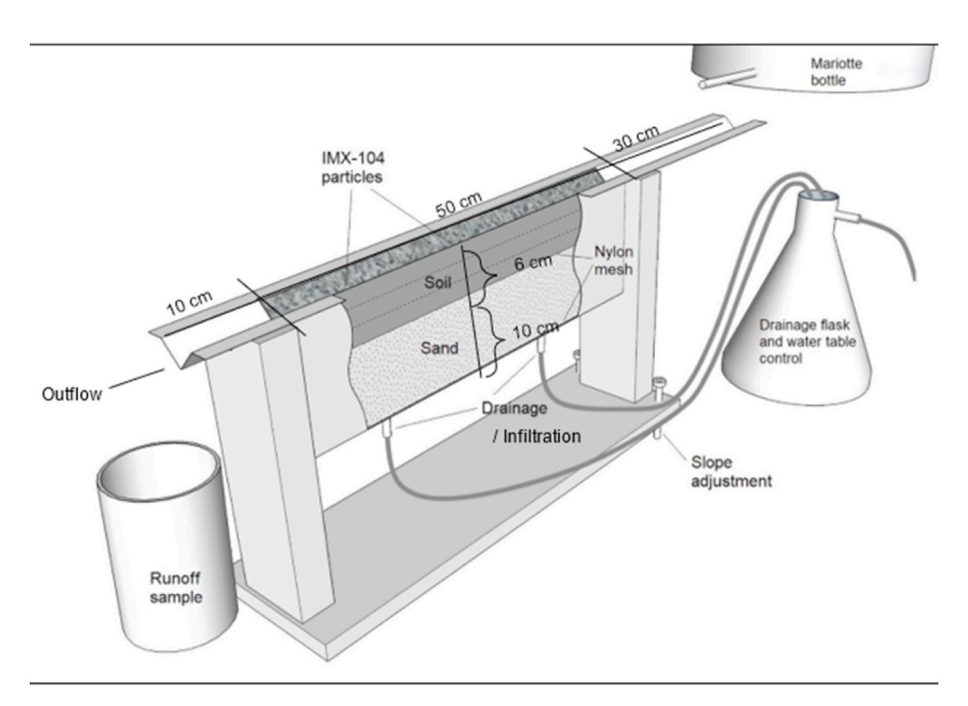


Fig. 1. Experimental setup for rill experiments.

above the lower boundary of the soil layer to maintain saturation and facilitate overland flow.

After saturation, the slope of the rill was adjusted to 5% as seen in other flume studies (Nearing et al., 1997; Nouwakpo et al., 2010).

The designed treatments for this experiment included a single 5% slope gradient, four particle sizes (4.75-9.51 mm, 2.83-4.75 mm, 2–2.83 mm, and <2 mm), and three flow rates (165-, 265-, and 300-mL min⁻¹). The particle size ranges were determined by available fractions from sieving residues from detonations conducted by CRREL (Bigl et al., 2020). Flow rates were decided based on pre-experiments trials. Flow less than 165 mL min⁻¹ produced limited particle movement, while flow above 300 mL min⁻¹ resulted in almost instant particle flushing. The goal was to have incremental increase in particle movement with increase in particle size. Each flow rate - particle size paring was replicated three times for a total of 36 runs. RO water was applied to the soil surface for 5 min at 400 mL min⁻¹ in the initial stage of the experiment ("rill formation"). Rill formation led to the creation of a more natural rill and the presence of natural features compared to the previously smooth packed rill. The flow was then stopped to uniformly place a target amount of 0.152 g of IMX-104 particles of one of the studied sizes onto the surface of the rill. The mean amount placed was $0.152 \pm 6.82 \times 10^{-4}$ g. The applied amount was similar to the density of energetics deposition found on training ranges in the vicinity of detonation sites where within in 10 m, 2.6-6.3 g were deposited on the surface (Bigl et al., 2021). A flow rate of 50 mL min⁻¹ was then applied to the rill for 5 min and an outflow sample was collected during this time. The purpose of this step was to imitate early rainfall and flow that would occur at the beginning of a rainfall event. After this "pre-wetting", the "treatment" flow was started. The flow velocity for each flow rate was measured using black dye as a tracer in a separate set of experiments to avoid contamination of the samples with the dye (Figure s1).

Outflow samples were collected in pre-weighed jars at the end of the flume. Ten samples were collected per run over a 15-min interval. A 15-min experiment duration was selected because in pre-trail runs the movement of particles was not observed past this time point. The first five samples were collected every minute, while the last five samples were collected every 2 min. Infiltration samples were collected and weighed at the same times as the outflow samples but were then combined into one container for the whole run for later analysis. The jars containing outflow and the infiltration container were weighed after sample collection. Once the run was complete, the soil pore water was drained and collected, and the soil was sampled in layers. Video was recorded throughout the experiment to track movement of the particles. Fig. 2 includes pictures of large particles that were taken before and after the experiment was completed.

For soil sampling, the top layer was defined as the surface of the rill to 2 cm deep, the second layer was a depth of 2–4 cm, and the third layer was a depth of 4–6 cm. After the top layer was collected, it was weighed and spread out to air dry for 48–72 h. Samples were air dried to prevent exposure of energetic residues to high temperatures in the oven. After drying, the soil was weighed again and then ground using a puck mill (Labtech Essa LM-2) before analysis. Grinding the sample with a puck mill is necessary to ensure representative subsampling for analysis when

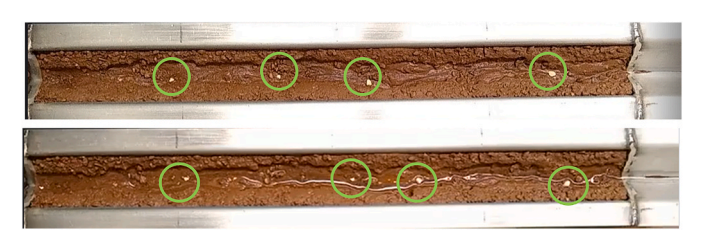


Fig. 2. The movement of large particles in the rill experiment. Before (top) and after (bottom) applied flow rate of 165 mL min^{-1} . The circles indicate the location of the particles. Direction of flow is left to right.

energetic particles are present as described in EPA Method 8330B (US EPA, 2006). The second and third layers of soil were weighed and then mixed thoroughly to ensure homogeneity. Two 5 g subsamples (approximately 4 g dry weight) per replicate were then collected from the second and third layers for analysis. The outflow was transferred from jars into centrifuge tubes and centrifuged at 3396 g for 20 min. After centrifugation, the supernatant was subsampled with a syringe and filtered through 0.45 μm PTFE filters into amber vials for high-performance liquid chromatography (HPLC) analysis and 45 mL of the remaining filtrate were archived. The remaining unfiltered solution was decanted leaving behind the sediment: transported soil and undissolved formulation particles and their fragments.

The extraction method for the transported sediment and the soil layers was the same. The extraction was done in two steps: first methanol and then 50/50 (v/v) methanol/water (Crouch et al., 2019). This extraction method was developed to complement EPA method 8330B to include IM compounds and products. For every 1 g of soil based on dry weight, 5 mL of solvent were added in each step. For extraction, we assumed 20% moisture content in the sediment based on the average measured values of sediment samples during pre-tests. For samples with less than 1 g of dry soil, 5 mL of solvent were used. After the addition of the solvent, the samples were put on a shaker at 120 rpm overnight and then centrifuged. The supernatant was sampled into amber vials for HPLC analysis. HPLC analysis followed methods of Arthur et al. (2018). After the second extraction, the samples were oven dried to determine dry weight of the sediment. The first (top) layers of the soil containing particles were processed using the same two step extraction but after the soil was ground. After the first layers or the surface layers were oven dried, their mass was found to be within 0.01 g from their air-dried mass.

The extraction efficiency was $101\pm4.9\%$ for DNAN (n = 33), $91\pm1.2\%$ for NTO (n = 19), $75\pm6.1\%$ for RDX (n = 25), and $40\pm4.6\%$ for HMX (n = 14) with a total IMX-104 mass of energetics ranging from 9×10^{-4} to 0.1216 g. The extraction efficiency for RDX with lower total particle mass up to $\sim\!0.022$ g (equivalent to $\sim\!2.6$ mg of RDX) was $99\pm7.8\%$ (n = 12). In our study, over 96% of our samples contained less than 2.6 mg of RDX. In Crouch et al. (2019) soils were spiked with 20 mg/kg of the 24 tested compounds with an average recovery of $102\pm5.75\%$ DNAN, $84\pm3.45\%$ NTO, $81\pm5.40\%$ RDX, and $73.5\pm4.88\%$ HMX. They flagged recoveries below 57% and above 135%.

HPLC samples were analyzed on an Thermo Scientific Dionex Ultimate 3000 HPLC with diode array detection (ThermoFisher, MA). All analyzed compounds were compared with standards, prepared in the same matrix as the corresponding samples, in terms of retention time and UV-Vis spectrum. The methods were adapted from Arthur et al. (2018). NTO analysis was conducted with a Hypercarb column (4.6 mm \times 150 mm, 5 μ m; ThermoFisher Scientific, MA, USA) at 34 °C. The injection volume was 20 μL and an isocratic method was used with a flow rate of 1 mL min⁻¹, a run time of 5 min, and an eluent composition of 75/25 (v/v) acetonitrile/deionized water with 0.1% trifluoroacetic acid. NTO was analyzed at 300 nm and eluted at 2.6 min. DNAN and RDX analysis was conducted with an Acclaim Explosives E2 column (4.6 mm \times 250 mm, 5 µm; ThermoFisher Scientific, MA, USA) at 34 °C. The injection volume was 20 µL and an isocratic method was used with a flow rate of 1 mL min⁻¹, a run time of 22 min, and an eluent composition of 43/57 (v/v) methanol/deionized water. Compounds were analyzed at the following wavelengths and eluted at the following retention times: 254 nm (HMX 7.1 min, RDX 11.2 min, DNAN 19.1 min).

The minimum detection limit (MDL) in water was 1.02 ppm for NTO, 1.02 ppm for HMX, 0.51 ppm for DNAN, and 0.67 ppm for RDX. The MDL in methanol was 1.36 ppm for NTO, 0.75 ppm for HMX, 0.84 ppm for DNAN, and 1.08 ppm for RDX. The MDL in the 50/50 (v/v) methanol/water was 0.64 ppm for NTO, 0.58 ppm for HMX, 1.52 ppm for DNAN, and 1.34 ppm for RDX. Standards were made up from pure solid pieces of the individual components provided by China Lake. The solids were dissolved in acetonitrile and then were used to spike the different

extraction solvents (water, methanol, methanol H/water) to develop 7-point calibration curves of 0.5 ppm-100 ppm.

3. Results

3.1. Flow characterization and sediment transport

Based on equation (1) defined by Bagnold (1966) for stream power and equation (2) by Yalin (1963) for shear stress, slope, velocity, and flow rate are the key parameters that influence sediment transport. In our study the slope was kept constant. Velocity depends on the total discharge (flow rate) and stream geometry. Since the rill experiments were performed under the same conditions, their geometry did not change, making flow velocity directly proportional to the flow rate (Fig. 3a, P = 0.00041). From this it can be expected that flow rate would be the primary factor that influences soil sediment yield (mass of sediment moved per time), as has been observed in several field studies (Nearing et al., 2007; Polyakov et al., 2010; Simanton et al., 1993), and potentially, energetic particle movement. In agreement with this, we did observe a significant (P = 0.02) positive relationship between flow rate and sediment yield (Fig. 3b).

3.2. Transport of energetic constituents

Transport in solution and sediment was observed for the energetic constituents of IMX-104 at each flow rate. The transport of the constituent compounds depended not only on flow rate but also the size of the particles that were placed on the surface. Multivariate analysis of variance (MANOVA) showed that for all constituent compounds the particle size had significant effect on each transport pathway, while flow rate only significantly influenced the amount found in sediment and amount remaining on the surface (Table s1). For mass found in the sediment, DNAN (p-value = 0.033, slope = 0.53), RDX (p-value = 0.0097, slope =

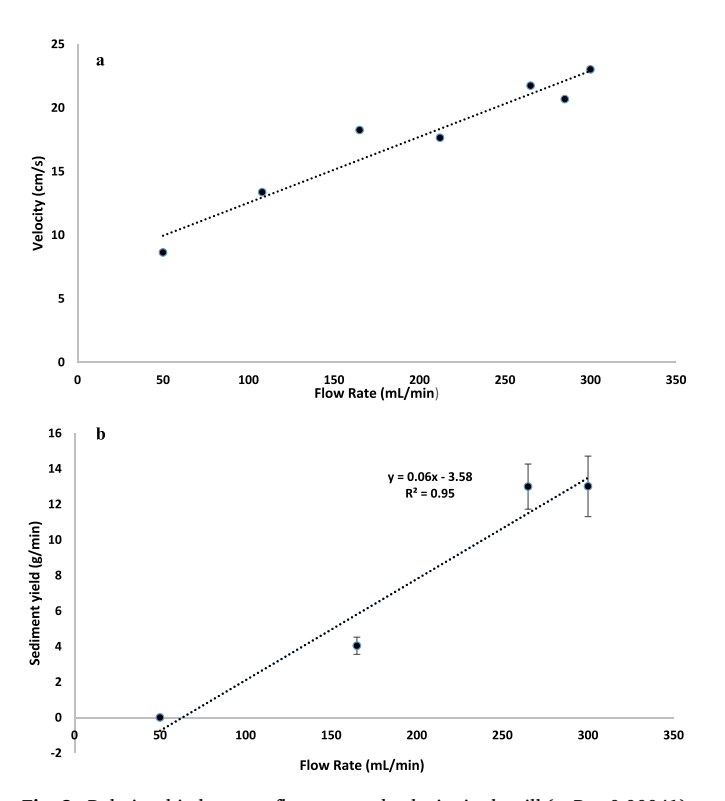


Fig. 3. Relationship between flow rate and velocity in the rill (a, P=0.00041). Relationship between flow rate and sediment yield (b, P=0.02). Additional flow rates were used to establish the relationship in panel a to decrease the uncertainty that can arise with fewer points.

0.189), and HMX (p-value = 0.012, slope = 0.0136) had a significant positive relationship with sediment yield while the more soluble NTO did not (plots not shown). The combined total mass of all energetic constituents recovered in sediment also had a significant positive relationship with sediment yield (Figure s2). The concentration of energetics in sediment are a combination of energetics that are translocated and adsorbed to soil particles.

The potential pathways of IMX-104 constituent transport was dissolution followed by movement in runoff or infiltration, and transport of particles with the eroding sediment. The amount of the constituent compounds found in solution originated from the dissolution of IMX-104 particles. Over the 15-min run, NTO had the largest percent (32 \pm 3%) of mass originally put on the surface moved into solution, as averaged across all flow rates and particle sizes, with the largest percent (60 \pm 10%) moved for small particles at 300 mL min⁻¹ (Table s2). RDX had the smallest percent mass transported in solution during the experiment with an average of 2.8 \pm 0.6% and highest of 9.6 \pm 0.8% for very small particles at 165 mL min⁻¹. The movement in solution for DNAN had an average value of 8 \pm 1%. The largest percent moved in solution for DNAN was 24 \pm 1% for very small particles at 165 mL min⁻¹. At higher flow rates, more of the energetic particles were transported sooner off the rill leaving less to dissolve over time to enter solution. For HMX the average percent mass found in solution was 6 \pm 1% with the highest value being found with very small particles at 300 mL min⁻¹ with a value of 22 \pm 6%.

DNAN had the largest percent mass moved in sediment over the 15-min run with an average percent mass of 22.0 \pm 3.6%. For NTO, the average percent transported in sediment was the smallest, 8 \pm 2%, with the largest amount being found at 265 mL min $^{-1}$ with medium particles, 28 \pm 12%. For RDX, the total average in sediment was 14.0 \pm 2.3% and the largest percent mass in sediment was 30 \pm 7% at 300 mL min $^{-1}$ with very small particles. The largest percent moved in sediment for HMX was 23.0 \pm 2.3% for small particles at 265 mL min $^{-1}$ flow rate with a total average of 9.0 \pm 1.6%.

The cumulative plots of energetics transport in solution and sediment over time (Figs. 4-6, and s3) indicate that there is an initial sharp increase of the constituent compound found in solution and sediment followed by a stage of steady state. Amounts of energetics both in solution and sediment coming from very small particles were higher than for other treatments starting from the "pre-wet" step, or time 0, because they can be mobilized even by the smallest flow rate used during this stage. With an increase in particle size, in general, less of all compounds was transported in solution; but there was no consistent trend for transport in solution with the flow rate. With time, the amount transported in solution decreased for all compounds (Figs. 4.1, 5.1, 6.1, and s3.1), and RDX from large particles was below the detection limit. Both RDX and DNAN reached a point when they were no longer appreciably dissolved but continued to be transported with the sediment. At low flow rates, highly soluble NTO was primarily found in solution because NTO was rapidly dissolving from the particles (Fig. 4.1A-C). For RDX, the transport in sediment increased for all particle sizes as the flow rate increased, while for NTO and DNAN this trend was only found for very small particles, and for HMX in small and medium particles. For NTO, DNAN, and HMX, although not linear, from the lowest flow rate to the higher two, the amount transported in sediment increased. Increase in transport in sediment would be expected because with increased flow rate there would be an increase in the shear stress.

Observed trends were interaction of particle size, flow rate, and properties of the compounds. Much greater differences were found between very small particles and all other particle sizes at all flow rates in solution for RDX, DNAN, and HMX, compared to NTO. A significant difference was also found in the percent mass transported in sediment for very small particles compared to all other particle sizes at 165 mL min⁻¹ for RDX, DNAN, and HMX (Figs. 5.2A and 6.2A, and s3.2A), but at higher flow rates the differences were smaller. The difference between how these compounds were transported in solution and sediment is seen

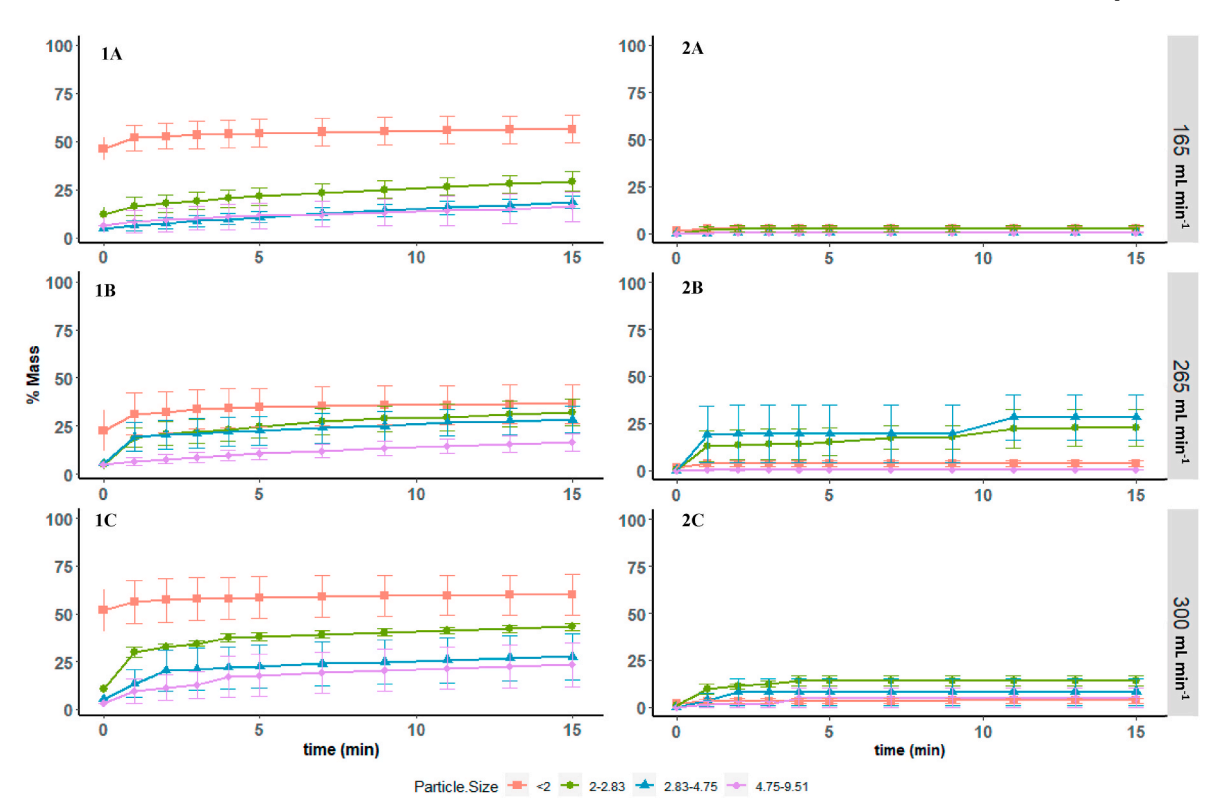


Fig. 4. Cumulative mass percent in solution (1A-C) and sediment (2A-C) for NTO. Error bars equal one standard error.*.

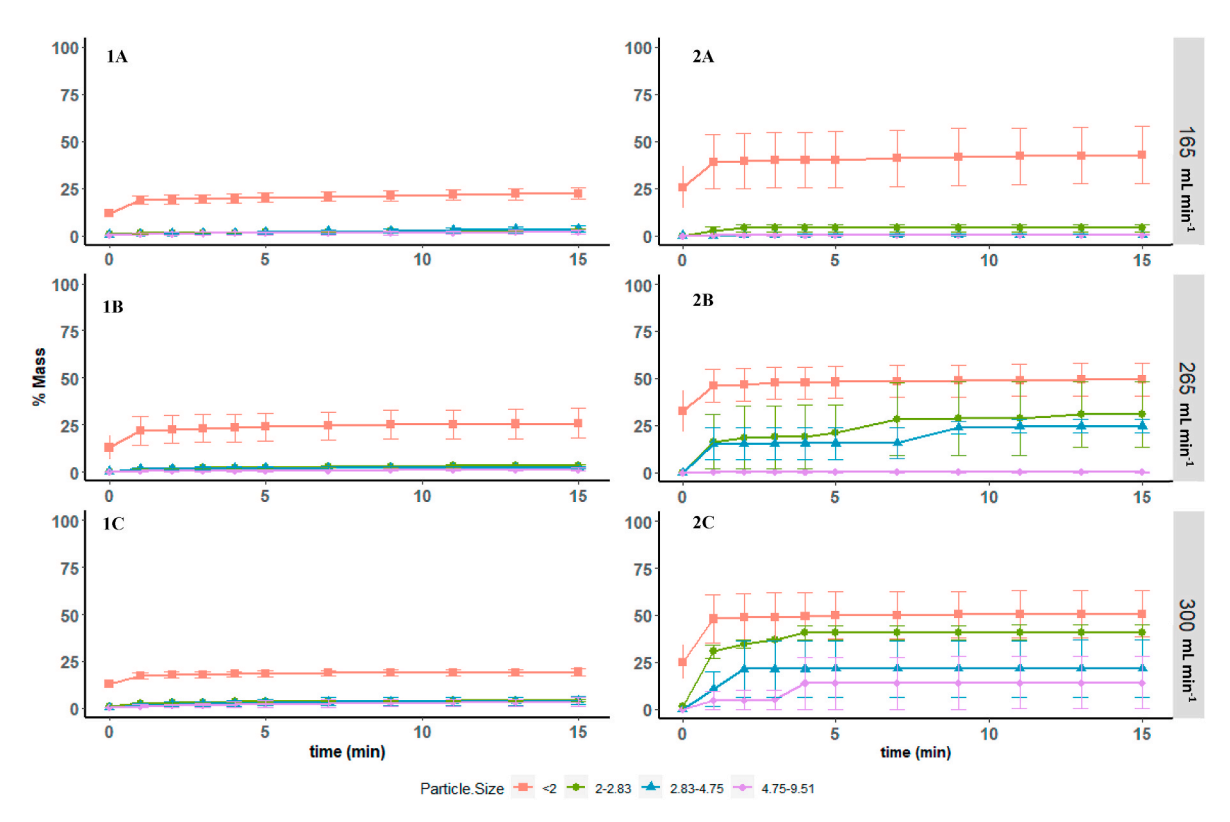


Fig. 5. Cumulative percent mass in solution (1A-C) and sediment (2A-C) for DNAN. Error bars equal one standard error.*.

when comparing Figs. 4.1, 5.1, and 6.1 and Figs. 4.2, 5.2, and 6.2. The solution transport increases steadily as particles dissolve, while transport in sediment appears to be more stepwise due to discrete movement of individual particles.

At 300 mL min⁻¹ for very small particles, HMX transport in solution continued to increase through the duration of the experiment (Figure s3.1C). Since it was expected that the majority of very small particles at this flow rate would be carried off in the first few minutes,

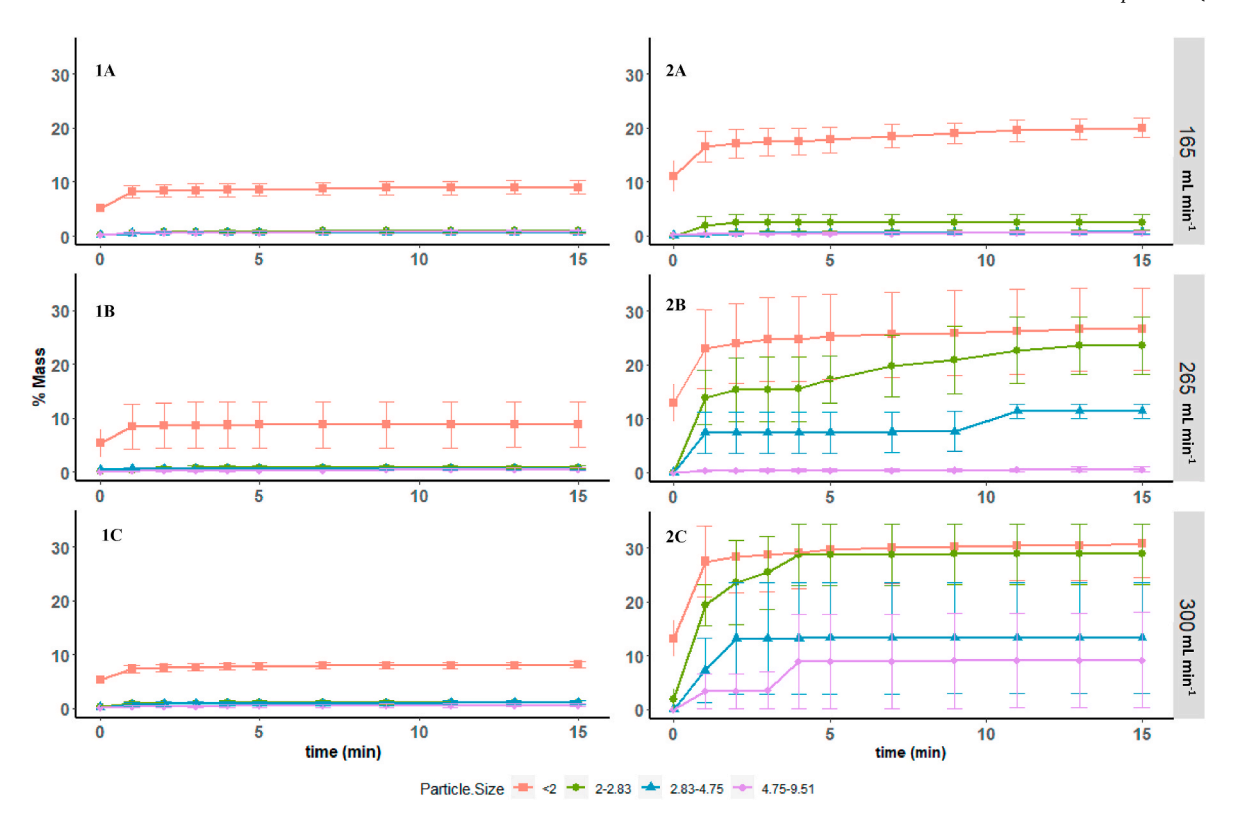


Fig. 6. Cumulative percent mass in solution (1A-C) and sediment (2A-C) for RDX. Error bars equal one standard error.*.

the continuous increase at the later time suggests that the higher flow rate may desorb HMX that was adsorbed to the surface, or the higher flow rate allows for greater dissolution of the remaining HMX particles.

The transport of NTO was dominated by dissolution; more was transported in solution than in sediment across all particle sizes (Fig. 7, Table s2). For very small and small sized particles, the major pathway for NTO transport was in solution (43.0 \pm 3.8%), while the majority of NTO in medium and large particles remained on the surface (54.0 \pm 4.1%). For very small particles, higher transport in infiltration was observed at 165 mL min $^{-1}$ (30 \pm 11%) compared to 265 mL min $^{-1}$ (8.0 \pm 2.4%) and 300 mL min⁻¹ (11.0 \pm 1.5%). Comparisons between pathways were determined by averaging values over all flow rates (Table s3). There was a significant increase in the amount of NTO in sediment comparing very small and small particles at 300 mL min⁻¹ and comparing medium and large particles at 265 mL min⁻¹. NTO had a significant difference between very small and all other particle sizes for transport in infiltration, solution, and sediment. A significant difference was observed between small and large particles for solution and surface, and for sediment between very small and small. Between medium and large particles, the only significant difference observed for NTO was in the sediment at 265 mL min⁻¹. The amount of NTO found in solution was significantly higher compared to DNAN, HMX, and RDX for all particle sizes.

The transport of DNAN and RDX was dominated by movement in the sediment compared to solution (Fig. 7, Table s2). Significantly more RDX was found in sediment than in solution for all particles sizes but large, while for DNAN difference was significant only for very small and small particles. For very small and small particles, the majority of added DNAN was transported in the sediment (34.0 \pm 4.8%), while for medium and large particles DNAN largely remained on the surface (51.0 \pm 4.4%). The majority of RDX (62 \pm 3.6%) remained on the surface for all but very small particles, for which sediment transport dominated (25.0 \pm 3.6%): differences were significant for all but small particles. Comparing transport in sediment between different particle sizes, a significant difference was found between very small and medium

particles and very small and large particles for both DNAN and RDX. For very small particles, significantly more RDX and DNAN were transported in solution than remained on the surface and the opposite was true for larger particle sizes. The percent of RDX in solution differed among all particle sizes except between large and medium particles, with the largest amount observed for the smallest particles. When comparing particle sizes averaged over all flow rates (Table s3), DNAN has significantly higher transport in solution for very small particles compared to all other sizes and significantly higher transport in sediment for very small particles compared to medium and large particles.

For HMX, it was observed that for the very small particles, transport was similar in sediment and in solution at 165 mL min⁻¹ and 265 mL \min^{-1} flow rates (13.78% and 14.78% in sediment and 14.06% and 10.70% in solution, respectively) while at 300 mL min⁻¹, the two transport routes were different with more transported in solution (14.36% in sediment and 21.98% in solution). Between sediment and solution transport pathways, HMX was found only to have a significant difference for small particles. The majority of HMX remained on soil surface except for very small particles. HMX had a significant difference between the percent found in solution vs. on the surface as well as in sediment vs. on the surface for all particle sizes. HMX was significantly different between very small and all other particle sizes in solution and on the surface. No significant difference was found between medium and large particles across all pathways. For the sediment, there was only significant difference when comparing particle sizes between very small and small particles and small and large particles.

Infiltration was the largest for RDX, DNAN, and NTO for very small particles with its highest value observed for NTO reaching 27.81% at 165 mL min $^{-1}$. Infiltration for HMX was highest for small particles at 165 mL min $^{-1}$ (21.29%). Infiltration only had significant difference for NTO and when comparing very small particles to other particle sizes. During the experiment infiltration rates were low (1.07 \pm 0.04 mL min $^{-1}$) resulting in the total amount of 45.0 \pm 6.3 g per run.

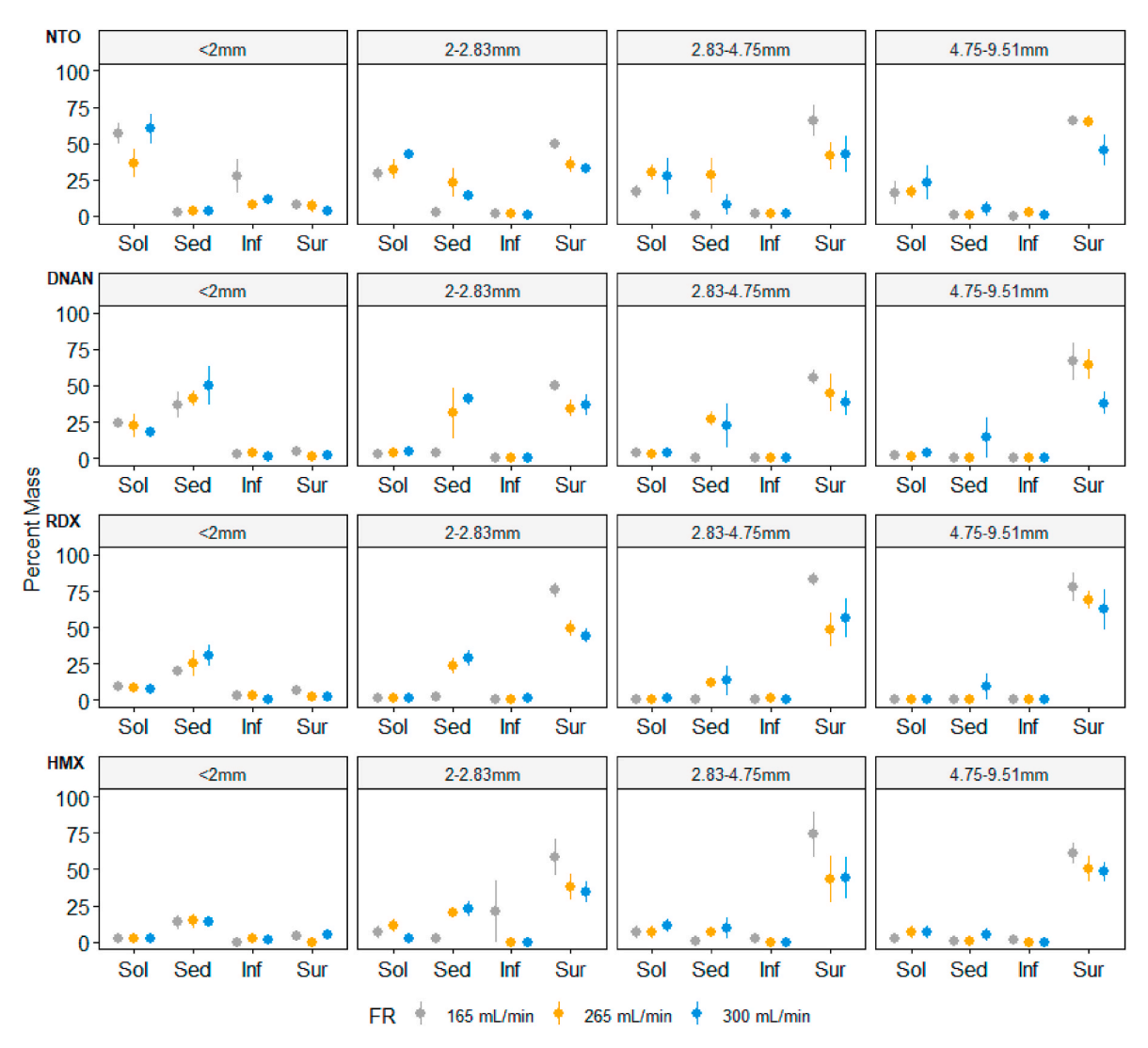


Fig. 7. Mass balance for NTO, DNAN, RDX, and HMX found in solution (Sol), sediment (Sed), infiltration (Inf), and on the surface (Sur). The colors correspond to the flow rate 165 mL min⁻¹ (gray), 265 mL min⁻¹ (orange), and 300 mL min⁻¹ (blue). The error bars are standard error. In this graph, an outlier for percent of DNAN in sediment for small particles at 265 mL min⁻¹ was removed as it was multiple standard deviations above the other replicates.*

4. Discussion

The transport rate of all energetic compounds was inversely correlated with their particle size. As flow rate increased, more RDX, HMX, and DNAN were transported with the sediment and less remained on the surface. The shear force that would be required to move particles increases with particle size. Thus, movement only occurred for larger particles at the higher flow rates. For large particles (4.75–9.51 mm) 300 mL min⁻¹ was the only flow rate able to cause considerable transport in the sediment. There were instances when no particle movement was observed, yet IM constituents were detected in the runoff sediment. This can be attributed to surface shedding and fracturing of original particles to produce small pieces, which could be further easily transported by the flow (Taylor et al., 2015). Significant differences were found between the amount remaining on the surface and transported in sediment for all constituent compounds at medium and large particle sizes. Since soil sediment yield and the mass of IMX-104 found in sediment had statistically significant positive correlation (P-value = 0.023; Figure s2) it can be expected that erosion can be used to understand IMX-104 transport. However due to the low correlation, using this relation directly for prediction of transport would be difficult.

Transport due to infiltration was found to be generally small except for NTO dissolving from very small particles. This was likely a combined effect of having a higher percent clay and a high water table and therefore low infiltration rate into the soil, low solubility, and high adsorption to soil for DNAN, RDX, and HMX making it unlikely that the energetics would reach into lower layers of the soil during the short experiment.

For NTO, as flow rate increased, the amount of it in solution generally increased, as can be expected given its high solubility. However, the trend was not consistent across all studied flow rates. This lack of continuous increase of NTO in solution transport with flow rate is contrary to the expectations that increasing flow leads to more abrasion and a larger volume of water which would increase the amount that is dissolved. One possible explanation for this could be that higher flow rates increase the transport of energetics with the sediment limiting the amount left on the surface to undergo dissolution. Another possible explanation is that due to drop impingement, described by Taylor et al. (2009), spatially isolated particles can hold a \sim 0.1 mm thick water film which can saturate with energetic particles between impinging raindrops, could impact the amount of energetic that was collected at the end of the rill.

Beyond the very small particles, there were few significant differences when comparing transport between particle sizes and flow rates. When comparing NTO to DNAN, RDX, and HMX, significantly more was found in solution for almost all flow rates and particle sizes. At the same

time, for very small particles at all flow rates, amounts of DNAN and RDX in sediment were significantly greater than NTO. This is consistent with NTO having much greater solubility compared to DNAN, RDX, and HMX, leaving more of NTO in solution and more of the other compounds in the sediment. When looking at the impact of flow rate, DNAN and RDX were found to primarily differ significantly in solution, while DNAN and HMX were found to primarily differ in the amount transported in sediment. Amounts of RDX and HMX were only significantly different in solution at 300 mL min⁻¹ for very small particles.

The reported amount of energetics in the sediment is a combined value of the amount adsorbed to the soil sediment and the amount in the formulation particles, or their pieces that were transported with the soil. The percent adsorbed relative to the amount in sediment was determined using reported K_d values for NTO and DNAN in Florence soil 0.06 and 1.9, respectively (Arthur et al., 2017; Mark et al., 2016) and calculated based on $f_{\rm oc}$ for RDX and HMX 0.816 and 1.03 respectively (Brannon and Pennington, 2002; Tucker et al., 2002). Measured $f_{\rm oc}$ for Florence soil was 0.0026. We estimated that 1.55% of NTO, 4.60% of DNAN, 1.02% of RDX, and 2.91% of HMX was transported adsorbed to the soil particles, therefore most of the contribution in sediment being transported comes from energetic particles.

The findings of this study carry implications for how IMX-104 would behave in the field. When IMX-104 is detonated, it breaks into various sizes. The amount of each particle size can vary by detonation (Bigl et al., 2020; Taylor et al., 2015). A majority of particles in Bigl et al. (2020) were found to be <2 mm with none being larger than 4.75 mm, whereas both Pennington et al. (2008) and Taylor et al. (2015) observed <2 mm particles as well as particles larger than 12.5 mm. Taylor et al. (2015) explain potential conditions for an explosive that can cause variability in particle size. Knowing this distribution, the major concern for ranges would be the smaller particle sizes as they are more likely to dissolve and move with the soil sediment. For these smaller sizes, there was more transport and dissolution meaning greater potential for contamination of nearby waterways or uptake by plants (Dodard et al., 2013; Kiiskila et al., 2015; Price et al., 2011; Schroer et al., 2017; Yoon et al., 2002). The concern for the larger particles that are less common is that they have very low transport and we would expect the less soluble constituents (DNAN, HMX, RDX) to remain on the surface and slowly dissolve (Arthur et al., 2018; Dontsova et al., 2014; Morley et al., 2006; Richard and Weidhaas, 2014) and biodegrade (Indest et al., 2017; Karthikeyan and Spain, 2016), whereas the more soluble NTO would remain on the surface longer but still dissolve with rainfall events and enter solution easily (Richard and Weidhaas, 2014). However, given a high enough flow rate, these particles that reside on the surface can be transported with the overland flow bringing greater instantaneous concentrations to nearby surface waters.

5. Conclusion

Based on the findings of this study, the transport of IMX-104 was dependent on the properties of the constituent compounds (NTO, DNAN, HMX, and RDX), the size of the particles, and the flow rate of water. The transport of NTO was dominated by dissolution while DNAN, HMX, and RDX were generally transported with the sediment. This reflects the higher solubility of NTO in water compared to DNAN, HMX, and RDX. For flow rates of 300 mL min $^{-1}$ or less, or a stream flow of 2.45 \times $10^{-3\frac{kgm}{s}}$ or less, movement of particles larger than 2.83 mm was limited and $56\pm4.12\%$ of initially placed mass remained on the surface for all compounds. The flow rate did not have a statistically significant impact on the amount of energetics in solution, but it did impact the amount of compounds found in sediment and remaining on the surface.

This research highlights the various transport pathways that can occur during overland flow, revealing the influence that particle size and flow rate both have on IMX-104 transportation in overland flow. This opens the door to future research into the potential impacts IMX-104

residues and other energetic contaminants have when transported in overland flow. One potential future area of interest would be to see if these contaminants can accumulate in the soil after being deposited from runoff. Another, to predict the fate and transport of munitions in overland flow.

Author contribution statement

Benjamin Karls: Methodology, Conceptualization, Software, Validation, Formal analysis, Investigation, Writing – original draft, Visualization. Katerina Dontsova: Methodology, Conceptualization, Validation, Writing – review & editing, Supervision, Funding Acquisation. Stephan Mercer Meding: Validation, Investigation, Writing – review & editing. Li Li: Methodology, Conceptualization, Investigation, Writing – review & editing. Viktor Polyakov: Methodology, Conceptualization, Validation, Investigation, Writing – review & editing. Warren Kadoya: Methodology, Investigation, Resources, Writing – review & editing. Samuel Beal: Investigation, Resources, Writing – review & editing.

Declaration of competing interest

The authors declare that they have no known competing financial interests or personal relationships that could have appeared to influence the work reported in this paper.

Data availability

Data will be made available on request.

Acknowledgements

This study was funded through SERDP under project ER19-1074. The authors are grateful to Kim Birdsall for her help in collecting soil that was used in the experiments; Mr. Matthew Bigl, Principal Investigator of ESTCP project ER18-5105, for providing the energetic residues; Mark Nearing for providing support during design of the experiment; and Favianna Cubello (University of Arizona) for assisting in the processing of samples. The authors are also grateful to anonymous reviewers and their suggestions in improving this paper.

Appendix A. Supplementary data

Supplementary data to this article can be found online at https://doi.org/10.1016/j.chemosphere.2022.136866.

References

- Arthur, J.D., Mark, N.W., Taylor, S., Šimunek, J., Brusseau, M.L., Dontsova, K.M., 2017. Batch soil adsorption and column transport studies of 2,4-dinitroanisole (DNAN) in soils. J. Contam. Hydrol. 199, 14–23. https://doi.org/10.1016/j.jconhyd.2017.02.004.
- Arthur, J.D., Mark, N.W., Taylor, S., Šimůnek, J., Brusseau, M.L., Dontsova, K.M., 2018. Dissolution and transport of insensitive munitions formulations IMX-101 and IMX-104 in saturated soil columns. Sci. Total Environ. 624, 758–768. https://doi.org/10.1016/j.scitotenv.2017.11.307.
- Bagnold, R.A., 1966. An Approach to the Sediment Transport Problem from General Physics. U.S. Government Printing Office. https://books.google.com/books?id=G09 6igXqR74C.
- Bigl, M., Beal, S., Ramsey, C., 2021. Determination of Residual Low-Order Detonation
 Particle Characteristics from IMX-104 Mortar Rounds.
- Bigl, M., Beal, S., Walsh, M., Ramsey, C., Burch, K., 2020. Sieve Stack and Laser Diffraction Particle Size Analysis of IMX-104 Low-Order Detonation Particles. https://doi.org/10.21079/11681/35515.
- Boddu, V.M., Abburi, K., Maloney, S.W., Damavarapu, R., 2008. Thermophysical properties of an insensitive munitions compound, 2,4-dinitroanisole. J. Chem. Eng. Data 53 (5), 1120–1125. https://doi.org/10.1021/je7006764.
- Brannon, J., Pennington, J., 2002. Environmental Fate and Transport Process Descriptors for Explosives, vol. 64.
- Cadwalader, G.O., Renshaw, C.E., Jackson, B.P., Magilligan, F.J., Landis, J.D., Bostick, B. C., 2011. Erosion and physical transport via overland flow of arsenic and lead bound

- to silt-sized particles. Geomorphology 128 (1–2), 85–91. https://doi.org/10.1016/j.geomorph.2010.12.025.
- Clausen, J.L., Korte, N., 2011. Fate and transport of energetics from surface soils to groundwater. In: Chappell, M.A., Price, C.L., George, R.D. (Eds.), Environmental Chemistry of Explosives and Propellant Compounds in Soils and Marine Systems: Distributed Source Characterization and Remedial Technologies, vol. 1069. American Chemical Society, pp. 273–316. https://pubs.acs.org/doi/abs/10.1021 /bk-2011-1069.ch015.
- Crouch, R., Smith, J., Stromer, B., Hubley, C., Beal, S., Lotufo, G., Butler, A., Wynter, M., Ro-Sado, D., Russell, A., Coleman, J., Clausen, J., Giordano, B., Montgomery, M., Bednar, A., 2019. Development and Optimization of Analytical Methods for Simultaneous Determination of IM and Legacy Explosive Compounds SERDP ER-2722 USACE ERDC-EL 1, -CRREL 2, and NRL 3 Final Report.
- Deng, H., Fei, Sun, Z., Zhang, Y., Fan, Ni, 2019. Phosphorus loss through overland flow and interflow from bare weathered granite slopes in southeast China. Sustainability 11, 4644. https://doi.org/10.3390/su11174644.
- Dodard, S.G., Sarrazin, M., Hawari, J., Paquet, L., Ampleman, G., Thiboutot, S., Sunahara, G.I., 2013. Ecotoxicological assessment of a high energetic and insensitive munitions compound: 2,4-Dinitroanisole (DNAN). J. Hazard Mater. 262, 143–150. https://doi.org/10.1016/j.jhazmat.2013.08.043.
- Dontsova, K., Taylor, S., Pesce-Rodriguez, R., Brusseau, M., Arthur, J., Mark, N., Walsh, M., Lever, J., Šimůnek, J., 2014. Dissolution of NTO, DNAN, and Insensitive Munitions Formulations and Their Fates in Soils, p. 92.
- Dontsova, K.M., Hayes, C., Pennington, J.C., Porter, B., 2009. Sorption of high explosives to water-dispersible clay: influence of organic carbon, aluminosilicate clay, and extractable iron. J. Environ. Qual. 38 (4), 1458–1465. https://doi.org/10.2134/jeq2008.0183.
- Douglas, T.A., Walsh, M.E., Weiss, C.A., McGrath, C.J., Trainor, T.P., 2012. Desorption and transformation of nitroaromatic (TNT) and nitramine (RDX and HMX) explosive residues on detonated pure mineral phases. Water, Air, Soil Pollut. 223 (5), 2189–2200. https://doi.org/10.1007/s11270-011-1015-2.
- Fuller, M.E., Schaefer, C.E., Andaya, C., Fallis, S., 2015. Production of particulate Composition B during simulated weathering of larger detonation residues. J. Hazard Mater. 283, 1–6. https://doi.org/10.1016/j.jhazmat.2014.08.064.
- Glover, D.J., Hoffsommer, J.C., 1973. Thin-layer chromatographic analysis of HMX in water. Bull. Environ. Contam. Toxicol. 10 (5), 302–304. https://doi.org/10.1007/bf01604820
- Guo, Z., Ma, M., Cai, C., Wu, Y., 2018. Combined effects of simulated rainfall and overland flow on sediment and solute transport in hillslope erosion. J. Soils Sediments 18 (3), 1120–1132. https://doi.org/10.1007/s11368-017-1868-0.
- Haderlein, S.B., Weissmahr, K.W., Schwarzenbach, R.P., 1996. Specific adsorption of nitroaromatic explosives and pesticides to clay minerals. Environ. Sci. Technol. 30 (2), 612–622. https://doi.org/10.1021/es9503701.
- Hawari, J., Monteil-Rivera, F., Perreault, N.N., Halasz, A., Paquet, L., Radovic-Hrapovic, Z., Deschamps, S., Thiboutot, S., Ampleman, G., 2015. Environmental fate of 2,4-dinitroanisole (DNAN) and its reduced products. Chemosphere 119, 16–23. https://doi.org/10.1016/j.chemosphere.2014.05.047.
- Hyer, K.E., 2001. Atrazine Transport through an Agricultural Watershed University of Virginial. ProQuest Dissertations and Theses.
- Indest, K., Hancock, D., Crocker, F., Eberly, J., Jung, C., Blakeney, G., Brame, J., Chappell, M., 2017. Biodegradation of insensitive munition formulations IMX101 and IMX104 in surface soils. J. Ind. Microbiol. Biotechnol. 44 (7), 987–995. https://doi.org/10.1007/s10295-017-1930-3
- Ju, K.-S., Parales, R.E., 2010. Nitroaromatic compounds, from synthesis to biodegradation. Microbiol. Mol. Biol. Rev.: MMBR (Microbiol. Mol. Biol. Rev.) 74 (2), 250–272. https://doi.org/10.1128/MMBR.00006-10.
- Kar, C., Lee, M., Stenstrom, M., 1996. Competitive Adsorption of Cyclotrimethylenetrinitramine (RDX) and Cyclotetramethylenetetranitramine (HMX).
- Karthikeyan, S., Spain, J.C., 2016. Biodegradation of 2,4-dinitroanisole (DNAN) by Nocardioides sp. JS1661 in water, soil and bioreactors. J. Hazard Mater. 312, 37–44. https://doi.org/10.1016/j.jhazmat.2016.03.029.
- Kiiskila, J.D., Das, P., Sarkar, D., Datta, R., 2015. Phytoremediation of explosive-contaminated soils. Curr. Pollut. Rep. 1 (1), 23–34. https://doi.org/10.1007/s40726-015-0003-3
- Mark, N., Arthur, J., Dontsova, K., Brusseau, M., Taylor, S., 2016. Adsorption and attenuation behavior of 3-nitro-1,2,4-triazol-5-one (NTO) in eleven soils. Chemosphere 144, 1249–1255. https://doi.org/10.1016/j. chemosphere.2015.09.101.

- Mark, N., Arthur, J., Dontsova, K., Brusseau, M., Taylor, S., Šimůnek, J., 2017. Column transport studies of 3-nitro-1,2,4-triazol-5-one (NTO) in soils. Chemosphere 171, 427–434. https://doi.org/10.1016/j.chemosphere.2016.12.067.
- Morley, M.C., Yamamoto, H., Speitel, G.E., Clausen, J., 2006. Dissolution kinetics of high explosives particles in a saturated sandy soil. J. Contam. Hydrol. 85 (3–4), 141–158. https://doi.org/10.1016/j.jconhyd.2006.01.003.
- Nearing, M.A., Nichols, M.H., Stone, J.J., Renard, K.G., Simanton, J.R., 2007. Sediment yields from unit-source semiarid watersheds at Walnut Gulch. Water Resour. Res. 43 (6) https://doi.org/10.1029/2006wr005692 n/a-n/a.
- Nearing, M.A., Norton, L.D., Bulgakov, D.A., Larionov, G.A., West, L.T., Dontsova, K.M., 1997. Hydraulics and erosion in eroding rills. Water Resour. Res. 33 (4), 865–876. https://doi.org/10.1029/97WR00013.
- Nouwakpo, S.K., Huang, C.-h., Bowling, L., Owens, P., 2010. Impact of vertical hydraulic gradient on rill erodibility and critical shear stress. Soil Sci. Soc. Am. J. 74 (6), 1914–1921. https://doi.org/10.2136/sssaj2009.0096.
- Olmstead, L.B., 1930. A Pipette Method of Mechanical Analysis of Soils Based on Improved Dispersion Procedure, p. 23 ill.; 23 cm.-USDA. https://handle.nal.usda.gov/10113/CAT86200164.
- Pennington, J.C., Silverblatt, B., Poe, K., Hayes, C.A., Yost, S., 2008. Explosive residues from low-order detonations of heavy artillery and mortar rounds. Soil Sediment Contam.: Int. J. 17 (5), 533–546. https://doi.org/10.1080/15320380802306669.
- Polyakov, V.O., Nearing, M.A., Nichols, M.H., Scott, R.L., Stone, J.J., Mcclaran, M.P., 2010. Long-term runoff and sediment yields from small semiarid watersheds in southern Arizona. Water Resour. Res. 46 (9) https://doi.org/10.1029/ 2009wr009001 n/a-n/a.
- Price, C.B., Brannon, J.M., Yost, S.L., Hayes, C.A., 2001. Relationship between redox potential and pH on RDX transformation in soil-water slurries. J. Environ. Eng. 26–21
- Price, R.A., Bourne, M., Price, C.L., Lindsay, J., Cole, J., 2011. Transport of RDX and TNT from composition-B explosive during simulated rainfall. In: ACS Symposium Series. American Chemical Society, pp. 229–240. https://doi.org/10.1021/bk-2011-1069.ch013.
- Richard, T., Weidhaas, J., 2014. Dissolution, sorption, and phytoremediation of IMX-101 explosive formulation constituents: 2,4-dinitroanisole (DNAN), 3-nitro-1,2,4-triazol-5-one (NTO), and nitroguanidine. J. Hazard Mater. 280, 561–569. https://doi.org/10.1016/j.jhazmat.2014.08.042.
- Schroer, H.W., Li, X., Lehmler, H.-J., Just, C.L., 2017. Metabolism and Photolysis of 2,4-Dinitroanisole in <i>Arabidopsis</i>. Environ. Sci. Technol. 51 (23), 13714–13722. https://doi.org/10.1021/acs.est.7b04220.
- Simanton, J.R., Osterkamp, W.R., Renard, K.G., 1993. Sediment Yield in a Semiarid Basin: Sampling Equipment Impacts.
- Spear, R.J., Louey, C.N., Wolfson, M.G., 1989. A Preliminary Assessment of 3-Nitro-1,2,4-Triazol-5-One (NTO) as an Insensitive High Explosive. MRL-TR-89-18). https://apps.dtic.mil/docs/citations/ADA215063.
- Taylor, S., Dontsova, K., Walsh, M., Walsh, M., 2015. Outdoor dissolution of detonation residues of three insensitive munitions (IM) formulations. Chemosphere 134, 250–256. https://doi.org/10.1016/j.chemosphere.2015.04.041.
- Taylor, S., Lever, J.H., Fadden, J., Perron, N., Packer, B., 2009. Outdoor weathering and dissolution of TNT and Tritonal. Chemosphere 77 (10), 1338–1345. https://doi.org/ 10.1016/j.chemosphere.2009.09.040.
- Tucker, W.A., Murphy, G.J., Arenberg, E.D., 2002. Adsorption of RDX to soil with low organic carbon: laboratory results, field observations, remedial implications. Soil Sediment Contam.: Int. J. 11 (6), 809–826. https://doi.org/10.1080/ 20025891107104.
- Us EPA, O.R.D., 2006. EPA Method 8330B (SW-846): Nitroaromatics, Nitramines, and Nitrate Esters by High Performance Liquid Chromatography (HPLC) [Data and Tools]. https://www.epa.gov/esam/epa-method-8330b-sw-846-nitroaromatics-nitramines-and-nitrate-esters-high-performance-liquid.
- Wang, C., Lazouskaya, V., Fuller, M.E., Caplan, J.L., Schaefer, C.E., Jin, Y., 2011. Dissolution of microscale energetic residues in saturated porous media: visualization and quantification at the pore-scale by spectral confocal microscopy. Environ. Sci. Technol. 45 (19), 8352–8358. https://doi.org/10.1021/es201649k. Yalin, M.S., 1963. An expression for bed-load transportation. J. Hydraul. Div. 89 (3), 29.
- Yalin, M.S., 1963. An expression for bed-load transportation. J. Hydraul. Div. 89 (3), 29.
 Yang, C.T., 1979. Unit stream power equations for total load. J. Hydrol. 40 (1), 123–138. https://doi.org/10.1016/0022-1694(79)90092-1.
- Yoon, J.M., Oh, B.-T., Just, C.L., Schnoor, J.L., 2002. Uptake and leaching of octahydro-1,3,5,7-tetranitro-1,3,5,7- tetrazocine by hybrid poplar trees. Environ. Sci. Technol. 36 (21), 4649–4655. https://doi.org/10.1021/es020673c.
- Zhang, K., Xuan, W., Yikui, B., Xiuquan, X., 2021. Prediction of sediment transport capacity based on slope gradients and flow discharge. PLoS One 16 (9), e0256827. https://doi.org/10.1371/journal.pone.0256827.